JACC: CARDIOVASCULAR IMAGING VOL. 4, NO. 12, 2011

ISSN 1936-878X/$36.00

PUBLISHED BY ELSEVIER INC.

DOI:10.1016/j.jcmg.2011.07.009

CVN Interview

Effects of Age, Diet, and Type 2 Diabetes on the Development and FDG Uptake of Atherosclerotic Plaques

Johanna M. U. Silvola, MSc,* Antti Saraste, MD, PhD,*† Iina Laitinen, PhD,§ Nina Savisto, MSc,* V. Jukka O. Laine, MD, PhD,‡ Suvi E. Heinonen, PhD,‖ Seppo Ylä-Herttuala, MD, PhD,‖ Pekka Saukko, MD, PhD,¶ Pirjo Nuutila, MD, PhD,* Anne Roivainen, PhD,*# Juhani Knuuti, MD, PhD*

Turku, Kuopio, and Helsinki, Finland; and Munich, Germany

OBJECTIVES This study investigated the effects of age, duration of a high-fat diet, and type 2 diabetes on atherosclerotic plaque development and uptake of ^{18}F-fluorodeoxyglucose (^{18}F-FDG) in 2 mouse models.

BACKGROUND The animal's age and start time and duration of a high-fat diet have effects on plaque composition in atherosclerotic mice.

METHODS The aortas of atherosclerotic low-density lipoprotein receptor deficient mice expressing only apolipoprotein B100 (LDLR$^{-/-}$ApoB$^{100/100}$) and atherosclerotic and diabetic mice overexpressing insulin-like growth factor II (IGF-II/LDLR$^{-/-}$ApoB$^{100/100}$) were investigated at 4, 6, and 12 months of age and older after varying durations of high-fat diet. C57BL/6N mice on normal chow served as controls. Plaque size (intima-to-media ratio), macrophage density (Mac-3 staining), and plaque uptake of ^{18}F-FDG were studied by means of in vivo positron emission tomography/computed tomography by ex vivo autoradiography and by histological and immunohistochemical methods.

RESULTS From the ages of 4 to 6 months and 12 months and older, the plaque size increased and the macrophage density decreased. Compared with the controls, the in vivo imaging showed increased aortic ^{18}F-FDG uptake at 4 and 6 months, but not at 12 months and older. Autoradiography showed focal ^{18}F-FDG uptake in plaques at all time points (average plaque-to-normal vessel wall ratio: 2.4 $\pm$ 0.4, $p < 0.001$) with the highest uptake in plaques with high macrophage density. There were no differences in the plaque size, macrophage density, or uptake of ^{18}F-FDG between LDLR$^{-/-}$ApoB$^{100/100}$ and IGF-II/LDLR$^{-/-}$ApoB$^{100/100}$ mice at any time point.

CONCLUSIONS The 6-month-old LDLR$^{-/-}$ApoB$^{100/100}$ and IGF-II/LDLR$^{-/-}$ApoB$^{100/100}$ mice demonstrated highly inflamed, large, and extensive atherosclerotic plaques after 4 months of a high-fat diet, presenting a suitable model for studying the imaging of atherosclerotic plaque inflammation with ^{18}F-FDG. The presence of type 2 diabetes did not confound evaluation of plaque inflammation with ^{18}F-FDG. (J Am Coll Cardiol Img 2011;4:1294–301) © 2011 by the American College of Cardiology Foundation

From the *Turku PET Centre, University of Turku and Turku University Hospital, Turku, Finland; †Department of Medicine, Turku University Hospital, Turku, Finland; ‡Department of Pathology, Turku University Hospital, Turku, Finland; §Nuklearmedizinische Klinik der Technischen Universität München, Munich, Germany; ‖A. I. Virtanen Institute for Molecular Sciences, University of Eastern Finland, Kuopio, Finland; ¶Department of Forensic Medicine, University of Turku, Turku, Finland; and the #Turku Center for Disease Modeling, University of Turku, Turku, Finland. The research leading to these results received funding from the European Union's Seventh Framework Program (FP7/2007-2013) for the Innovative Medicine Initiative under grant agreement No. IMI/115006 (the SUMMIT consortium); the Instrumentarium Foundation,

In mice deficient in low-density lipoprotein receptor (LDLR) and apolipoprotein B48, being able to synthesize only apolipoprotein B100 ($LDLR^{-/-}ApoB^{100/100}$), severe hypercholesterolemia with elevated levels of LDL cholesterol develops. This leads to extensive atherosclerosis that can be accelerated with a high-fat diet. The lipoprotein profile of $LDLR^{-/-}ApoB^{100/100}$ mice is highly atherogenic

See page 1302

and resembles that of human familial hypercholesterolemia better than any other mouse model currently available (1–3). Type 2 diabetes increases the predisposition to atherosclerosis and related cardiovascular diseases. A novel insulin-like growth factor II (IGF-II)/$LDLR^{-/-}ApoB^{100/100}$ mouse model overexpresses IGF-II in pancreatic β cells and shows characteristics of type 2 diabetes with no additional changes in the plasma lipoprotein fractions (1). In both mouse models, age at the start of a high-fat diet and the duration of the diet may have drastic effects on the development and composition of plaques (1), and therefore the optimal time point for studying the metabolic activity of plaques remains uncertain.

Positron emission tomography (PET) with ^{18}F-fluorodeoxyglucose (^{18}F-FDG) has been used to assess inflammation in atherosclerotic plaques because of its uptake by macrophages with active glucose metabolism (4,5). A strong ^{18}F-FDG signal in culprit carotid artery plaques in patients with recent stroke (6) and the correlation of ^{18}F-FDG uptake with macrophage density indicate that PET imaging with this tracer has the potential to identify vulnerable atherosclerotic plaques (7,8). However, the factors that determine ^{18}F-FDG uptake in atherosclerotic plaques still remain incompletely understood (9). Type 2 diabetes increases the predisposition to atherosclerosis and related cardiovascular diseases. Recent studies have shown that high ^{18}F-FDG uptake is frequently observed in individuals with impaired glucose tolerance and type 2 diabetes (10,11).

We report on the effects of age, duration of a high-fat diet, and type 2 diabetes on atherosclerotic plaque composition and metabolic activity assessed by ^{18}F-FDG uptake in 2 different mouse strains: $LDLR^{-/-}ApoB^{100/100}$ and IGF-II/$LDLR^{-/-}ApoB^{100/100}$.

METHODS

Animals and study design. All animal experiments were reviewed and approved by the Lab-Animal Care & Use Committee of the State Provincial Office of Southern Finland. A total of 30 $LDLR^{-/-}ApoB^{100/100}$ mice (strain #003000, The Jackson Laboratory, Bar Harbor, Maine) and 29 IGF-II/$LDLR^{-/-}ApoB^{100/100}$ mice (A. I. Virtanen Institute for Molecular Sciences, University of Eastern Finland, Kuopio, Finland) were used in the experiments. They were divided into 3 groups based on their age: 4, 6, and 12 months and older. The 4- and 6-month-old mice were fed with a Western-type diet (0.2% total cholesterol, TD 88137, Harlan Teklad, Harlan Laboratories, Madison, Wisconsin), starting at the age of 2 months until imaging. Older mice (≥12 months) were fed with the Western-type diet for 3 to 4 months before imaging. C57BL/6N mice (n = 15, age 7 to 14 months) fed with regular chow were used as controls. The characteristics of the studied animals are shown in Table 1.

The mice (N = 74) were fasted with ad libitum access to water for 4 h before the ^{18}F-FDG injection. Before the tracer injection, blood glucose levels were measured from the femoral vein with a glucometer (One Touch, UltraEasy, LifeScan, Inc., Milpitas, California). The ^{18}F-FDG (12 ± 3 MBq) was injected intravenously via a tail vein catheter in isoflurane-anesthetized mice. A subset of mice (n = 34) (Table 1) were imaged in vivo. After 90 min, the animals were killed, and the thoracic aorta was excised and rinsed in saline solution to remove blood. The aorta was frozen, and

ABBREVIATIONS AND ACRONYMS

$ApoB^{100/100}$ = mouse expressing only apolipoprotein B100

ARG = autoradiography

CT = computed tomography

^{18}F-FDG = ^{18}F-fluorodeoxyglucose

%IA/g = percentage of injected radioactivity per gram of tissue

IGF-II = insulin-like growth factor II

IMR = intima-to-media ratio

LDLR = low-density lipoprotein receptor

PET = positron emission tomography

PSL = photostimulated luminescence

ROI = region of interest

Helsinki, Finland; the Finnish Cultural Foundation, Helsinki, Finland; the Finnish Foundation for Cardiovascular Research, Helsinki, Finland; and the Aarne Koskelo Foundation, Helsinki, Finland. The studies were conducted within the Finnish Centre of Excellence in Molecular Imaging in Cardiovascular and Metabolic Research supported by the Academy of Finland, the University of Turku, the Turku University Hospital, and the Åbo Akademi University, and within the Turku Collegium for Science and Medicine of the University of Turku. Dr. Knuuti has consulted for Lantheus, Inc. All other authors have reported that they have no relationships relevant to the contents of this paper to disclose.

Manuscript received March 2, 2011; revised manuscript received July 6, 2011; accepted July 13, 2011.

Table 1 Basic Characteristics of Investigated Animals

	LDLR$^{-/-}$ApoB$^{100/100}$ Mice			IGF-II/LDLR$^{-/-}$ApoB$^{100/100}$ Mice			C57BL/6N
Age, months	4	6	12–17	4	6	12–15	7–14
High-fat diet, months	2	4	3–4	2	4	3	ND
No. of animals (F/M)	7 (7/0)	10 (1/9)	13 (2/11)	9 (7/2)	9 (6/3)	11 (5/6)	15 (0/15)
Weight, g*	23 ± 2	39 ± 7	41 ± 7	25 ± 6	32 ± 8	38 ± 4	38 ± 4
PET/CT, no.	3	3	9	2	3	8	6
IMR × macrophage, %, no. of animals†	6	9	3	5	9	8	ND

*Values are mean ± SD. †The intima-to-media ratio was measured from Movat staining and the percentage of intimal macrophages was quantified from Mac-3–stained aortic crosssections from the level of aortic ostia.
ApoB$^{100/100}$ = mouse expressing only apolipoprotein B100; CT = computed tomography; F/M = female/male; IGF-II = insulin-like growth factor II; IMR = intima-to-media ratio; LDLR = low-density lipoprotein receptor; ND = not done; PET = positron emission tomography.

sequential longitudinal 20- and 8-μm cryosections were cut with a cryomicrotome at −15°C and thaw-mounted onto microscope slides for autoradiography (ARG) studies. Radioactivity in the blood was measured with a gamma counter (Triathler 3", Hidex, Turku, Finland) that was cross-calibrated with a dose calibrator (VDC-202, Veenstra Instruments, Joure, the Netherlands), and the hearts were collected and preserved in formalin for further studies.

^{18}F-FDG PET/computed tomography. A dedicated small animal PET/computed tomography (CT) scanner (Siemens, Knoxville, Tennessee) was used for in vivo imaging 50 min after injection of 13 ± 4 MBq ^{18}F-FDG. PET images were acquired for 20 min, followed by CT angiography (20 min). To obtain vascular contrast, an iodinated intravascular contrast agent (Fenestra VC, Art Advanced Research Technologies Inc., Montreal, Quebec, Canada) was injected (0.2 ml) via a tail vein catheter without moving the animal. The mice were anesthetized with 1.5% isoflurane for injections and imaging. CT acquisition consisted of 272 projections with the exposure time of 1200 ms, x-ray voltage of 80 kVp, and anode current of 500 μA for a full 360° rotation. The PET and CT images were reconstructed with a filtered back-projection algorithm. Coregistration of PET and CT images was done using an automatic weighted mutual information algorithm and confirmed visually on the basis of anatomic landmarks. The intensity of in vivo ^{18}F-FDG uptake was quantified by measuring the percentage of injected radioactivity per gram of tissue (%IA/g) and corrected for injected radioactivity. The %IA/g was calculated by using the mean pixel activity value (kBq/ml) within the region of interest (ROI) placed on the aortic arch (oval ROI size, 2.1 mm^3) and brachiocephalic artery (cylinder ROI size, 1.3 mm^3) in the coronal PET/CT images, identified on the basis of the CT angiogram by using Inveon Research Workplace software (Siemens). The axial and sagittal views were used to ensure that the ^{18}F-FDG uptake was from the artery.

Autoradiography. The thoracic aortas of all mice (N = 74) were studied with ARG to determine the uptake of ^{18}F-FDG in atherosclerotic plaques and in healthy vessel wall, as described previously (11). Longitudinal 20- and 8-μm cryosections of the aorta were cut, air-dried for 5 min, and apposed to an imaging plate (Fuji Imaging Plate BAS-TR2025, Fuji Photo Film Co., Ltd., Tokyo, Japan). After an exposure time of 4 h, the imaging plates were scanned with Fuji Analyzer BAS-5000 (internal resolution of 25 μm). The 20-μm sections were stained with hematoxylin and eosin, and 8 to 10 sections from each mouse were examined for morphology under a light microscope. After a careful coregistration of the autoradiographs and hematoxylin and eosin images, ^{18}F-radioactivity was measured from the following ROIs: 1) noncalcified plaque (excluding media); 2) calcified area in plaque (excluding media); and 3) normal vessel wall (no lesion formation) (Fig. 1) and expressed as count densities (photostimulated luminescence [PSL]/mm^2) using Tina 2.1 software (Raytest Isotopemessgeräte, GmbH, Straubenhardt, Germany). The count densities of background radiation were subtracted from the actual ROI data, and the results for each mouse were normalized for injected radioactivity and decay. The analysis method has previously been reported to be reproducible (coefficient of variation of 2 independent observers: 4.5%) (12).

The 8-μm cryosections were stained with a rat anti-mouse Mac-3 antibody (Clone M3/84, 1:5000, BD Pharmingen, Franklin Lakes, New Jersey) as described previously (12) to compare the ^{18}F-FDG uptake and density of macrophages in atherosclerotic plaques. Based on a semiquantitative analysis of Mac-3 staining, the plaques were cate-

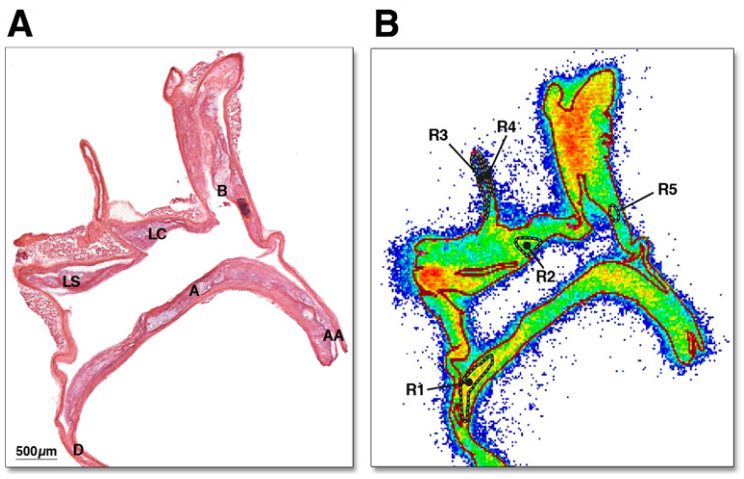

Figure 1. An Example of Autoradiography Analysis

(A) Hematoxylin-eosin image. **(B)** Coregistered autoradiograph and hematoxylin and eosin image (**red lines** represent the borders of the hematoxylin and eosin image) of the same section. R1 and R2 = regions of interest (ROIs) in plaque (noncalcified); R3 and R4 = ROIs in normal vessel wall; R5 = ROI in calcified plaque area. A = arch; AA = ascending aorta, B = brachiocephalic artery; D = descending thoracic aorta; LC = left common carotid artery; LS = left subclavian artery.

gorized into: 1) noninflamed (none or occasional Mac-3 stained macrophages); and 2) inflamed (occasional and some groups of macrophages or abundant infiltration of macrophages).

Histology and immunohistochemistry. To compare plaque areas (intima-to-media ratio [IMR]) and macrophage infiltration of plaques between groups, 5-μm serial sections of formalin-fixed and paraffin-embedded hearts were cut at the level of the aortic root and stained with anti-mouse Mac-3 or modified Movat's pentachrome stain (Table 1). The sections were evaluated under a light microscope, high-resolution digital photomicrographs were captured, and the areas of intima and media were limited by using image editing software (Adobe Photoshop cp, Adobe Systems, San Jose, California). The proportion of macrophages in the intima was determined from the Mac-3–stained sections, and the IMRs were calculated from the Movat-stained sections using automated image analysis software (Image-Pro Plus 5.0, Media Cybernetics, Silver Spring, Maryland). Furthermore, the IMR × macrophage (%) factor was used to describe the amount of macrophages compared with plaque size.

Statistical methods. All results are expressed as mean ± SD values. Comparisons of nonpaired data between 2 groups were made using a *t* test and between multiple groups using analysis of variance with Tukey's correction. A paired *t* test was used for comparing paired data between 2 groups. All analyses were performed with SAS software, version 9.1 (SAS Institute, Inc., Cary, North Carolina). Values of $p < 0.05$ were considered statistically significant.

RESULTS

Characterization of atherosclerotic plaques. No atherosclerosis was detected in the aortas of the control mice, whereas the atherosclerotic mice showed extensive atherosclerotic plaques, as seen in Figures 2A and 2B. Plaque size, given as the IMR, was comparable between the $LDLR^{-/-}ApoB^{100/100}$ and $IGF\text{-}II/LDLR^{-/-}ApoB^{100/100}$ mice, and it increased from 4 months to 6 and ≥12 months in both strains (Fig. 2C). Macrophage density was highest at 4 and 6 months of age and decreased by ≥12 months of age (Fig. 2D). As a result, the indicator of the total plaque macrophage number calculated as the IMR × macrophage (%) factor (Fig. 2E) was highest at 6 months of age in $IGF\text{-}II/LDLR^{-/-}ApoB^{100/100}$ mice and at both 6 and ≥12 months of age in $LDLR^{-/-}ApoB^{100/100}$ mice.

Blood ^{18}F-FDG uptake and glucose values. The ^{18}F-FDG radioactivity in blood was at the same level in the $LDLR^{-/-}ApoB^{100/100}$ (1.1 ± 0.4 IA%/g, pooled data, $p = 0.4$, compared with $IGF\text{-}II/LDLR^{-/-}ApoB^{100/100}$, $p = 0.2$, compared with C57BL/6N mice), $IGF\text{-}II/LDLR^{-/-}ApoB^{100/100}$ (1.2 ± 0.5 IA%/g, pooled data, $p = 0.5$ compared with C57BL/6N mice), and C57BL/6N control (0.9 ± 0.4 IA%/g) mice. No significant differences

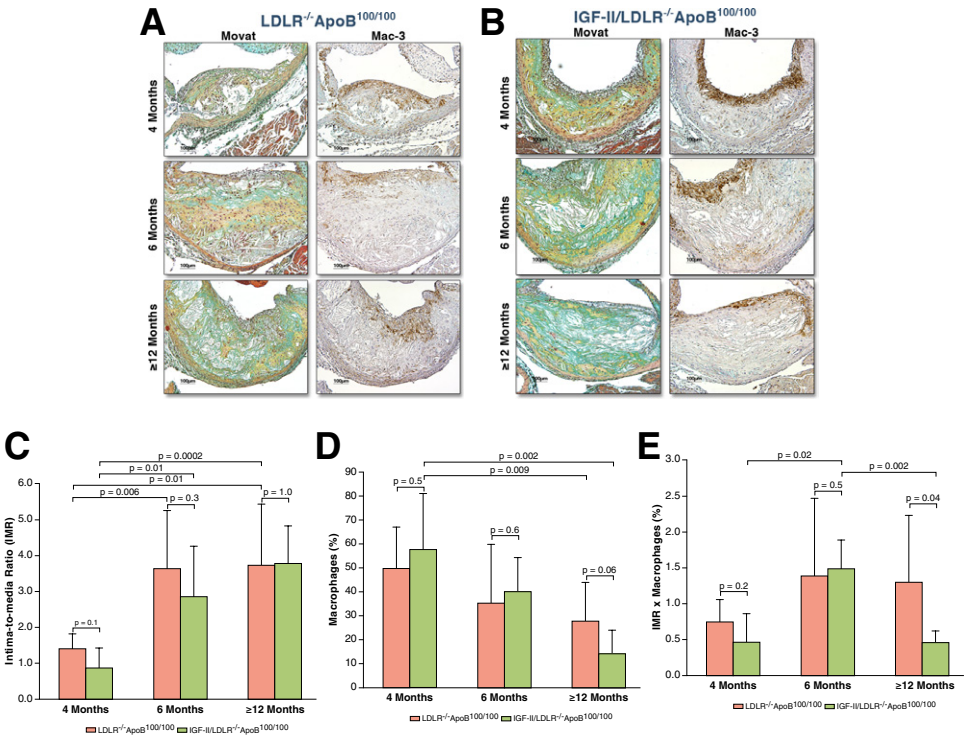

Figure 2. Characterization of Atherosclerosis Plaques of LDLR$^{-/-}$ApoB$^{100/100}$ and IGF-II/LDLR$^{-/-}$ApoB$^{100/100}$ Mice

Representative aortic root sections stained with Movat or anti-mouse Mac-3 immunohistochemistry from LDLR$^{-/-}$ApoB$^{100/100}$ **(A)** and IGF-II/LDLR$^{-/-}$ApoB$^{100/100}$ **(B)** mice at different ages. **(C)** Mean (± SD) intima-to-media ratios (IMR). **(D)** Percentage of Mac-3–stained intimal area. **(E)** Factor of IMR × proportion of macrophages (%) from aortic ostia. ApoB$^{100/100}$ = mouse expressing only apolipoprotein B100; IGF-II = insulin-like growth factor II; LDLR = low-density lipoprotein receptor.

were observed in blood glucose values between the LDLR$^{-/-}$ApoB$^{100/100}$ (7.2 ± 1.5 mmol/l), IGF-II/LDLR$^{-/-}$/ApoB$^{100/100}$ (6.9 ± 1.6 mmol/l) or C57BL/6N control (7.8 ± 1.8 mmol/l) mice after a 4-h fast.

^{18}F-FDG PET/CT. In vivo imaging demonstrated a focal ^{18}F-FDG signal in aortic arch and in brachiocephalic artery (Fig. 3). Compared with healthy control mice, the in vivo ^{18}F-FDG uptake in the aortic arch and brachiocephalic artery was significantly higher in the LDLR$^{-/-}$ApoB$^{100/100}$ mice at the age of 6 months ($p = 0.04$ and $p = 0.01$, respectively), and in the IGF-II/LDLR$^{-/-}$ApoB$^{100/100}$ mice at the age of 4 months ($p = 0.005$ and $p = 0.02$, respectively) and 6 months ($p = 0.01$ and $p = 0.01$, respectively). There were no significant differences in ^{18}F-FDG uptake between the LDLR$^{-/-}$ApoB$^{100/100}$ and IGF-II/LDLR$^{-/-}$ApoB$^{100/100}$ mice in any age group.

Autoradiography. Altogether 4,444 ROIs (2,469 from plaques and 1,975 from normal vessel walls) were analyzed from the 20-μm sections of atherosclerotic and control mice. Calcified plaques were seen in all mice 12 months and older (21% of analyzed plaques) and in 11 of 19 mice age 6 months (6% of analyzed plaques), but only in 1 LDLR$^{-/-}$ApoB$^{100/100}$ mouse age 4 months (2% of analyzed plaques). No differences were found in PSL/mm^2 for the ROIs between the noncalcified plaques and calcified areas in plaques (measured from the same animal), and therefore these data were pooled. As shown in Table 2, the uptake of ^{18}F-FDG was 2 to 2.4 times higher in atherosclerotic plaques than in the normal vessel wall ($p < 0.001$) in all groups of atherosclerotic mice. The uptake levels of ^{18}F-FDG in plaques and normal vessel walls were comparable between the LDLR$^{-/-}$ApoB$^{100/100}$ and IGF-II/LDLR$^{-/-}$ApoB$^{100/100}$ mouse strains and at different ages in both atherosclerotic strains. Furthermore, the uptake level of ^{18}F-FDG in the normal vessel wall was comparable between the atherosclerotic mice and healthy controls.

The uptake of ^{18}F-FDG was 1.7 ± 0.5 fold higher in inflamed (25 ± 14 PSL/mm^2, n = 354) than noninflamed (16 ± 12 PSL/mm^2, n = 92)

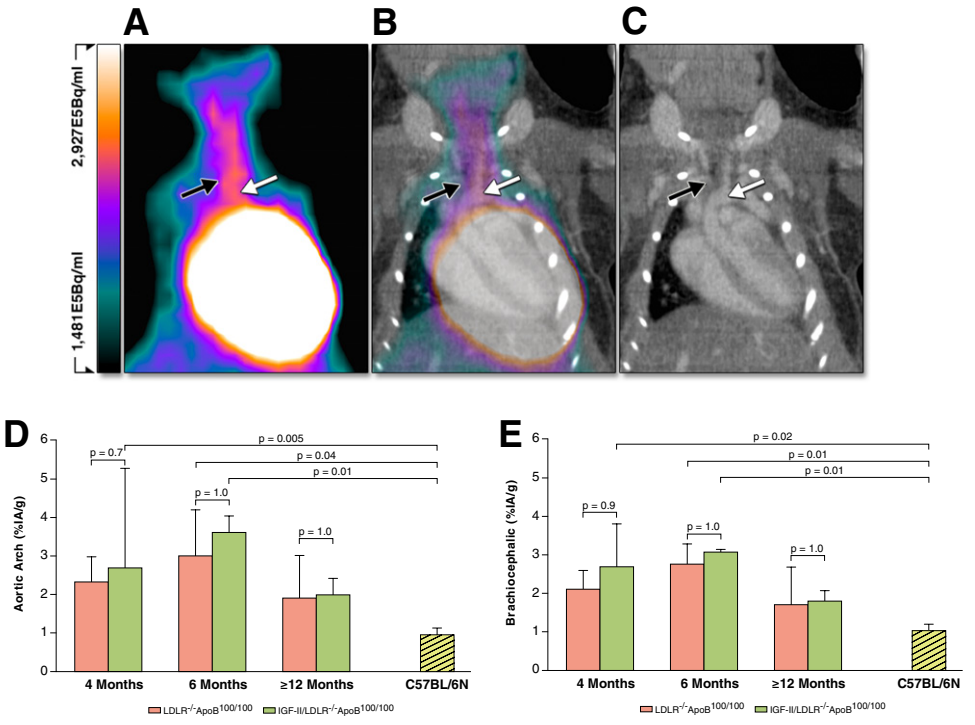

Figure 3. ^{18}F-FDG PET/CT Imaging

Representative in vivo PET **(A)**, CT angiography **(C)**, and fused PET/CT **(B)** images demonstrating ^{18}F-FDG signal in the aortic arch region. Average uptake of ^{18}F-FDG measured in the aortic arch **(white arrows in A–C)** **(D)** and brachiocephalic artery **(E)** **(black arrows in A–C)** in LDLR$^{-/-}$ApoB$^{100/100}$ and IGF-II/LDLR$^{-/-}$ApoB$^{100/100}$ mice expressed as percentage of injected radioactivity per gram of tissue (%IA/g) (mean ± SD). CT = computed tomography; ^{18}F-FDG = ^{18}F-fluorodeoxyglucose; PET = positron emission tomography; other abbreviations as in Figure 2.

plaques ($p < 0.0001$ [Fig. 4], pooled data from 6-month-old and 12-month and older LDLR$^{-/-}$ApoB$^{100/100}$ and IGF-II/LDLR$^{-/-}$ApoB$^{100/100}$ mice), as analyzed from the 8-μm anti-mouse Mac-3–stained sections. The 4-month-old mice were not included in the analysis because of lack of noninflamed plaques in these groups.

DISCUSSION

To date, ^{18}F-FDG is the best characterized tracer available for PET imaging, providing a noninvasive method for studying inflammation associated with atherosclerotic lesions (9,13). In the present study, we used ^{18}F-FDG to investigate the metabolic activity of atherosclerotic plaques in atherosclerotic LDLR$^{-/-}$ApoB$^{100/100}$ and diabetic as well as atherosclerotic IGF-II/LDLR$^{-/-}$ApoB$^{100/100}$ mice. There were no major differences in the vascular ^{18}F-FDG uptake and plaque development between the LDLR$^{-/-}$ApoB$^{100/100}$ and IGF-II/LDLR$^{-/-}$ApoB$^{100/100}$ mouse strains. The 6-month-old mice kept on a high-fat diet for 4 months demonstrated large and macrophage-rich atheromatous plaques. These mice can be considered particularly useful for the evaluation of new imaging agents for the detection

Table 2. Autoradiography Results of ^{18}F-FDG Uptake in Aortic Cryosections

	LDLR$^{-/-}$ApoB$^{100/100}$			IGF-II/LDLR$^{-/-}$ApoB$^{100/100}$		
Age, months	4	6	≥12	4	6	≥12
Plaque	69 ± 23	61 ± 34	71 ± 27	53 ± 21	59 ± 31	50 ± 26
Normal vessel wall	34 ± 8	29 ± 20	33 ± 13	24 ± 8	26 ± 14	21 ± 11
Ratio*	2.0 ± 0.3	2.3 ± 0.5	2.3 ± 0.5	2.2 ± 0.4	2.4 ± 0.4	2.4 ± 0.6
p Value†	<0.0006	<0.0002	<0.0001	<0.0002	<0.0003	<0.0003

Values are expressed as photostimulated luminescence/mm^2 (mean ± SD). *Plaque-to-normal vessel wall ratio. †Plaque versus normal vessel wall. Abbreviations as in Table 1.

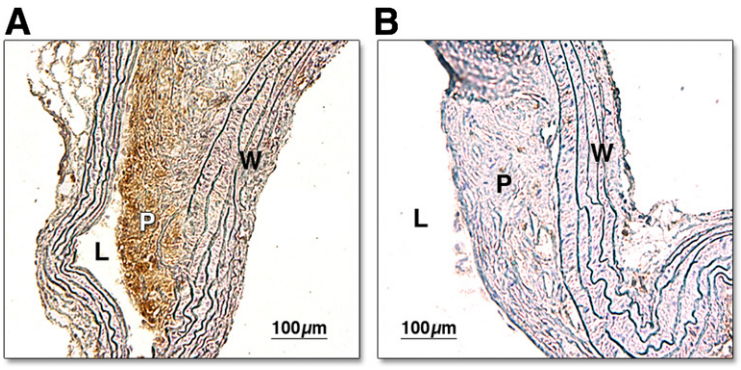

Figure 4. Colocalization of ^{18}F-FDG and Density of Macrophages in Atherosclerotic Plaques

Macrophages stained with anti-mouse Mac-3 **(brown color)** in inflamed plaque **(A)**, and noninflamed **(B)** plaque. L = lumen; P = plaque; W = wall; other abbreviation as in Figure 3.

of advanced atherosclerotic plaques. This was confirmed by the highest plaque uptake of ^{18}F-FDG shown both by in vivo PET/CT imaging and by ex vivo ARG.

Given that type 2 diabetes and impaired glucose tolerance, on the one hand, are associated with an increased risk of atherosclerotic cardiovascular events and, on the other hand, may have an influence on the uptake and kinetics of glucose analog ^{18}F-FDG (9–11), we aimed to investigate the effect of the diabetic background on vascular ^{18}F-FDG uptake in the IGF-II/LDLR$^{-/-}$ApoB$^{100/100}$ mice. The novel IGF-II/LDLR$^{-/-}$ApoB$^{100/100}$ mouse represents a promising model for studies of macrovascular complications in type 2 diabetes with insulin resistance, hyperglycemia, and mild hyperinsulinemia with a hypercholesterolemic background. In IGF-II/LDLR$^{-/-}$ApoB$^{100/100}$ mice, increased blood glucose values have been reported in the prolonged fasted state, whereas fed-state glucose levels were comparable to those of LDLR$^{-/-}$ApoB$^{100/100}$ mice (1). In the present study, both the LDLR$^{-/-}$ApoB$^{100/100}$ and IGF-II/LDLR$^{-/-}$ApoB$^{100/100}$ mice were fasted for 4 h and had equal blood glucose levels and showed similar distribution of ^{18}F-FDG in blood. Our result that plaque uptake of ^{18}F-FDG is comparable in the LDLR$^{-/-}$ApoB$^{100/100}$ and IGF-II/LDLR$^{-/-}$ApoB$^{100/100}$ mice indicates that the diabetic metabolism itself does not affect the feasibility of ^{18}F-FDG for imaging atherosclerotic plaques in these models. Furthermore, as to the plaque development, no significant differences were found between the LDLR$^{-/-}$ApoB$^{100/100}$ and IGF-II/LDLR$^{-/-}$ApoB$^{100/100}$ mice, suggesting that the lesion progression in these models is mainly dependent on increased cholesterol level after 2 to 4 months on a high-fat diet. As reported previously, sex seems to have no influence on plaque development in the LDLR$^{-/-}$ApoB$^{100/100}$ and IGF-II/LDLR$^{-/-}$ApoB$^{100/100}$ mice (1).

Although several mouse models have proved useful in atherosclerosis research, the occurrence of plaque rupture and thrombosis is extremely rare in mice. Nevertheless, the histology of atherosclerotic plaque development in mice and humans has more similarities than differences, and comparative genetics show that many mechanisms of murine and human atherogenesis are shared (14). Mouse plaques are particularly rich in macrophages, which allow the imaging of plaque inflammation, which is an important mechanism of plaque progression and a typical feature of plaques at high risk of rupture. In the present study, the highest ^{18}F-FDG signal in the aortic arch and brachiocephalic artery was detected in the 6-month-old LDLR$^{-/-}$ApoB$^{100/100}$ and IGF-II/LDLR$^{-/-}$ApoB$^{100/100}$ mice in which histology and immunohistochemical assessments demonstrated the highest IMR × macrophage (%) factor with the largest plaques, given as IMR, and the highest macrophage density. This is consistent with previous studies indicating that the highest uptake of ^{18}F-FDG is seen in the plaques with the highest macrophage density (15). After a 2-month high-fat diet, both the LDLR$^{-/-}$ApoB$^{100/100}$ and IGF-II/LDLR$^{-/-}$ApoB$^{100/100}$ mice demonstrated an extremely high proportion of infiltrated macrophages in plaques already at the age of 4 months. At this stage, however, the small size of the plaques limits their use in imaging studies. In mice 12 months and older and kept on a high-fat diet for 3 to 4 months, the plaques were characterized by large

areas of calcification and necrotic core, but a relatively low content of macrophages. Although ARG showed higher ^{18}F-FDG uptake in these plaques compared with the adjacent healthy vessel wall, the difference was not significant when atherosclerotic and healthy mice were compared using in vivo imaging. Therefore, these older mice are not recommended for studies that require a high degree of plaque inflammation. The average life span of a mouse is about 2 years, but the life expectancy and causes of death have not been reported for the mouse models used in the present study (16).

Study limitations. A limitation of our study is that we were not able to correct in vivo images for partial volume effects and quantitatively compare in vivo measurements with ARG or histology in the same atherosclerotic plaques. In vivo measurements were done in the arch region because of the most prominent plaque and a good angiography image in this region. To minimize the effect of tissue sampling and variable cutting plane of tissue sections on ARG measurements, results were averaged over multiple plaques in the thoracic aorta. Standardized sectioning through the aortic root was used for comparison of histological features in plaques between mice.

CONCLUSIONS

No differences were found between the age-matched LDLR$^{-/-}$ApoB$^{100/100}$ and IGF-II/LDLR$^{-/-}$ApoB$^{100/100}$ mice with regard to plaque development and composition. For the evaluation of new imaging agents for the detection of advanced atherosclerotic plaques, we recommend using at least 6-month-old mice fed a high-fat diet for 3 to 4 months before imaging. The presence of type 2 diabetes did not significantly influence the vascular uptake of ^{18}F-FDG in the IGF-II/LDLR$^{-/-}$ApoB$^{100/100}$ model.

Acknowledgments

The authors thank Erja Mäntysalo for excellent assistance in animal experiments, Erica Nyman and Liisa Lempiäinen for performing tissue sectioning and immunohistochemistry, and Irina Lisinen for providing expertise in statistical analyses.

Reprint requests and correspondence: Johanna M. U. Silvola, Turku PET Centre, Turku University Hospital, Kiinamyllynkatu 4-8, P.O. Box 52, FI-20520 Turku, Finland. *E-mail: johanna.silvola@utu.fi.*

REFERENCES

1. Heinonen SE, Leppanen P, Kholova I, et al. Increased atherosclerotic lesion calcification in a novel mouse model combining insulin resistance, hyperglycemia, and hypercholesterolemia. Circ Res 2007;101:1058–67.
2. Veniant MM, Zlot CH, Walzem RL, et al. Lipoprotein clearance mechanisms in LDL receptor-deficient "Apo-B48-only" and "Apo-B100-only" mice. J Clin Invest 1998;102:1559–68.
3. Veniant MM, Sullivan MA, Kim SK, et al. Defining the atherogenicity of large and small lipoproteins containing apolipoprotein B100. J Clin Invest 2000;106:1501–10.
4. Davies JR, Izquierdo-Garcia D, Rudd JHF, et al. FDG-PET can distinguish inflamed from non-inflamed plaque in an animal model of atherosclerosis. Intern J Cardiovasc Imaging 2010;26:41–8.
5. Tawakol A, Migrino RQ, Hoffmann U, et al. Noninvasive in vivo measurement of vascular inflammation with F-18 fluorodeoxyglucose positron emission tomography. J Nucl Cardiol 2005;12:294–301.
6. Moustafa RR, Izquierdo-Garcia D, Fryer TD, et al. Carotid plaque inflammation is associated with cerebral microembolism in patients with recent transient ischemic attack or stroke: a pilot study. Circ Cardiovasc Imaging 2010;3:536–41.
7. Tawakol A, Migrino RQ, Bashian GG, et al. In vivo F-18-fluorodeoxyglucose positron emission tomography imaging provides a noninvasive measure of carotid plaque inflammation in patients. J Am Coll Cardiol 2006;48:1818–24.
8. Rudd JH, Warburton EA, Fryer TD, et al. Imaging atherosclerotic plaque inflammation with [18F]-fluorodeoxyglucose positron emission tomography. Circulation 2002;105:2708–11.
9. Sheikine Y, Akram K. FDG-PET imaging of atherosclerosis: do we know what we see? Atherosclerosis 2010;211:371–80.
10. Tahara N, Kai H, Yamagishi S, et al. Vascular inflammation evaluated by [F-18]-fluorodeoxyglucose positron emission tomography is associated with the metabolic syndrome. J Am Coll Cardiol 2007;49:1533–9.
11. Kim TN, Kim S, Yang SJ, et al. Vascular inflammation in patients with impaired glucose tolerance and type 2 diabetes. Circ Cardiovasc Imaging 2010;3;142–8.
12. Haukkala J, Laitinen I, Luoto P, et al. Ga-68-DOTA-RGD peptide: biodistribution and binding into atherosclerotic plaques in mice. Eur J Nucl Med Mol Imaging 2009;36:2058–67.
13. Langer HF, Haubner R, Pichler BJ, Gawaz M. Radionuclide imaging: a molecular key to the atherosclerotic plaque. J Am Coll Cardiol 2008;52:1–12.
14. Bentzon JF, Falk E. Atherosclerotic lesions in mouse and man: is it the same disease? Curr Opin Lipidol 2010;21:434–40.
15. Zhao Y, Zhao S, Kuge Y, Strauss WH, Blankenberg FG, Tamaki N. Localization of deoxyglucose and annexin A5 in experimental atheroma correlates with macrophage infiltration but not lipid deposition in the lesion. Mol Imaging Biol 2011;13:712–20.
16. Jawień J, Nastałek P, Korbut R. Mouse models of experimental atherosclerosis. J Physiol Pharmacol 2004:55:503–17.

Key Words: atherosclerosis ■ diabetes ■ ^{18}F-fluorodeoxyglucose ■ mouse model ■ positron emission tomography.